Volume 1 | Number 1 | Jan 2013 | Pages 1–100

CrystEngComm

www.rsc.org/crystengcomm

www.rsc.org/crystengcomm

ARTICLE

Rational Design and Synthesis of a Series of 3D Lanthanide Metal-Organic Frameworks with Different Structures Driven by Reaction Conditions

Tingting Zhao, Lirong Zhang*, Dongmei Wang, Guanghua Li, Qisheng Huo, and Yunling Liu*

Abstract Twelve novel three-dimensional (3D) lanthanide metal-organic frameworks with formula $\{[LnK(C_4N_2O_4S)_2(H_2O)_2](H_2O)_{0.5}\}$ (Ln = La (**1**), Ce (**2**), Pr (**3**), Nd (**4**), Sm (**5**), Eu (**6**), Gd (**7**), Tb (**8**)), $\{[Ln_2K_2(C_4N_2O_4S)_2(C_4O_4H_2)_2(H_2O)_4](H_2O)\}$ (Ln = La (**9**), Ce (**10**)), and $\{[Ln_2(C_4N_2O_4S)_3(H_2O)](H_2O)\}$ (Ln = La (**11**), Ce (**12**)), are solvothermally synthesized by reaction of 1,2,5-thiadiazole-3,4-dicarboxylate (H_2tdc) ligand with corresponding lanthanide nitrate. These compounds exhibit three different types of structures which changed from nonporous to open-framework MOFs by modulating the reaction conditions. Compounds **1**-**8** (type I) with **moc** topology are constructed by 1D zigzag chains and pillared water molecules. While the Fumaric acid (Fac) as the coligand is introduced the reaction to replace the pillared water, and links the similar zigzag chains to assemble compounds **9** and **10** (type II) with **dia** topology. Compounds **11** and **12** (type III) with the chiral space group possess 1D right/left helical chains along *b* axis, and the helical chains alternatively link together to form 3D frameworks with new (3,4,5)-connected topology. The luminescent property study shows that compounds **5**, **6**, **8** display intense orange, red and green luminescence and exhibit the typical Sm^{3+}, Eu^{3+} and Tb^{3+} ion emission, respectively. Furthermore, compounds **1**, **7**, **9** and **11** also exhibit intense green and blue luminescence arising from the H_2tdc ligand.

Introduction

Progress in metal-organic frameworks (MOFs) is thriving for their desired characteristics and pore size via rational design.[1] These hybrid solids couple the variety of potential ligands from coordination chemistry with the topological diversity of solid-state chemistry, and their permanent porosity, high surface areas, fine-tunable pore structures, and adjustable chemical functionalities make them possess potential applications in gas adsorption and separation, ion exchange, magnetism, luminescence, and drug release.[2] Lanthanide based MOFs (Ln-MOFs), owing to their unique luminescent and magnetic properties arising from 4*f* electrons are good candidates to construct functional compounds with specific properties.[3] Their high coordination numbers and flexible coordination geometry produce varied connected modes, and Ln ions with appreciably different radii from La^{3+} (1.06 Å) to Lu^{3+} (0.85 Å) may generate different structures.[4] Hydrothermal or solvothermal conditions as the routine synthetic method for MOFs are easily affected by many factors, such as types of starting materials, solvent polarity and pH value, etc, which can influence the formation of the final product.[4b, 5] Therefore, according to the lanthanide contraction effect, subtly changing of relative molar ratio for the homologous compounds of lanthanides may exhibit various structures, it is important and effective route to construct diverse lanthanide compounds.[4a, 4c]

Generally, Ln ions have high affinity and prefer to bind to hard donor atoms, such as oxygen or hybrid oxygen-nitrogen atoms from multidentate ligands. The rigid 4,5-imidazoledicarboxylic acid (H_3imdc) ligand as excellent N, O donor, has been already proven to be efficient for construction of lanthanide-MOFs, and it is suitable for being antenna organic linker to sensitize the Ln^{3+}.[3b, 6] Whereas, 1,2,5-thiadiazole-3,4-dicarboxylate (H_2tdc) ligand, whose configuration is similar to H_3imdc, coordinating with lanthanide metal is still unexplored to date. Compared to the H_3imdc ligand, two carboxylate groups of H_2tdc ligand are easily to distort and cause the thiadiazole ring and carboxylate groups to be not in the same plane, which could enhance the ability of monodentate coordination and create more coordinated sites. Additionally, 2-site S of thiadiazole also provide potential coordination ability, the resultant configuration could produce diverse coordination modes. Moreover, because of the large radius of the S atom, its lone pair electrons can be easily delocalized within the thiadiazole leading to the ligand exhibits excellent charge-transfer capacity to target the luminescence of Ln-MOFs,[7] and the ligand itself is found to exhibit blue luminescence in the visible region. Therefore, utilizing H_2tdc ligand to construct Ln-MOFs may not only possess diverse structures, but also generate different types of luminescent properties. Herein, we report an intriguing example of the structural change for Ln-MOFs based on H_2tdc ligand driven by coligand, solvent polarity

and the value of pH. Compounds **1-12** are assembled in the similar reaction conditions. Compared with **1-8**, compounds **9-10** are synthesized by introducing the coligand Fumaric acid and modulating the relative molar ratio of $Ln(NO_3)_3 \cdot 6H_2O$ and H_2tdc ligand, while compounds **11-12** are synthesized by changing the solvent polarity and the value of pH, therefore, three different types of structures exhibite: $\{[LnK(C_4N_2O_4S)_2(H_2O)_2](H_2O)_{0.5}\}_n$ (Ln = La (**1**), Ce (**2**), Pr (**3**), Nd (**4**), Sm (**5**), Eu (**6**), Gd (**7**), Tb (**8**)) for type I with monoclinic system and space group $C2/_C$, $\{[Ln_2K_2(C_4N_2O_4S)_2(C_4O_4H_2)_2(H_2O)_4](H_2O)\}_n$ (Ln = La (**9**), Ce (**10**)) for type II with triclinic system and space group P-1, $\{[Ln_2(C_4N_2O_4S)_3(H_2O)](H_2O)\}_n$ (Ln = La (**11**), Ce (**12**)) for type III with monoclinic system and space group $P2_1$. Single crystal X-ray structures are determined for these compounds, and luminescent properties of compounds **1**, **5**, **6**, **7**, **8**, **9** and **11** are also assessed.

Experimental Section

Materials and methods

H_2tdc ligand was prepared according to the reported procedures in 80% yield.[8] All the other reagents of analytical grade were obtained from commercial sources and used without further purification. X-ray powder diffraction (XRD) data were collected on a Rigaku 2550 diffractometer with Cu Kα radiation (λ = 1.5418 Å). Elemental analysis was performed on a Perkin-Elmer 2400 element analyzer. Inductively coupled plasma (ICP) analyses were carried out on a Perkin-Elmer Optima 3300 Dv spectrometer. Infrared (IR) spectra were recorded within the 400-4000 cm^{-1} region on a Nicolet Impact 410 FTIR spectrometer using KBr pellets. The thermal gravimetric analyses (TGA) were performed on TGA Q500 thermogravimetric analyzer used in air with a heating rate of 10 ^oC min. Fluorescence spectra were collected on a Fluoromax-4 spectrophotometer for the solid powder samples at room temperature.

Synthesis of Compounds 1-8.

A mixture of $Ln(NO_3)_3 \cdot 6H_2O$ (Ln = La, Ce, Pr, Nd, Sm, Eu, Gd and Tb, 0.039 mmol), H_2tdc (0.100 mmol), KOH (0.100 mL, 0.56 M in water), and 2 mL of DMF/H_2O (1:1) was sealed in a 20 mL vial with the pH of 5.0 and heated at 85 ^oC for 12 h and 105 ^oC for 24 h. Block crystals were collected (70-80 % yield based on $Ln(NO_3)_3 \cdot 6H_2O$). The agreement between the experimental and simulated PXRD patterns indicated the phase-purity of as-synthesized product (see Supporting Information Figure S1), and the as-synthesized compounds **1-8** were insoluble in water and common organic solvents. ICP and elemental analysis (wt %) for **1**: Calcd: C, 16.93; H, 0.88; N, 9.87; S, 11.30, La, 24.48, K, 6.89. Found: C, 16.67; H, 0.83; N, 9.62; S, 10.98, La, 24.36, K, 6.76. For **2**: Calcd: C, 16.90; H, 0.88; N, 9.85; S, 11.28, Ce, 24.64, K, 6.87. Found: C, 16.76; H, 0.81; N, 9.66; S, 11.05, Ce, 24.32, K, 6.67. For **3**: Calcd: C, 16.82; H, 0.87; N, 9.83; S, 11.22, Pr, 24.71, K, 6.86. Found: C, 16.73; H, 0.85; N, 9.77; S, 11.13, Pr, 24.43, K, 6.72. For **4**: Calcd: C, 16.77; H, 0.86; N, 9.77; S, 11.13, Nd, 25.13, K, 6.82. Found: C, 16.91; H, 0.89; N, 10.37; S, 11.43, Nd, 25.32, K, 6.96. For **5**: Calcd: C, 16.53; H, 0.86; N, 9.67; S, 11.14, Sm, 25.91, K, 6.77. Found: C, 17.27; H, 0.89; N, 9.72; S, 11.22, Sm, 25.98, K, 6.80. For **6**: Calcd: C, 16.52; H, 0.86; N, 9.64; S, 11.13, Eu, 26.31, K, 6.78. Found: C, 16.16; H, 0.81; N, 9.37; S, 10.93, Eu, 26.43, K, 6.72. For **7**: Calcd: C, 16.36; H, 0.85; N, 9.53; S, 10.96, Gd, 26.82, K, 6.65. Found: C, 16.63; H, 0.89; N, 9.68; S, 10.98, Gd, 26.86, K, 6.77. For **8**: Calcd: C, 16.36; H,

0.85; N, 9.57; S, 10.86, Tb, 27.69, K, 6.61. Found: C, 16.56; H, 0.88; N, 9.65; S, 10.95, Tb, 27.96, K, 6.98. IR (KBr, cm^{-1}) for compound **1** (4000-400 cm^{-1}): 3515 (w), 3363 (br), 1630 (s), 1445 (s), 1368 (m), 1307 (s), 1092 (m), 797 (s), 535 (m), 478 (m) (IR for other compounds are shown in Figure S2).

Synthesis of Compounds 9-10.

A mixture of $Ln(NO_3)_3 \cdot 6H_2O$ (Ln = La and Ce, 0.039 mmol), H_2tdc (0.045 mmol), Fumaric acid (0.043 mmol), KOH (0.15 mL, 0.56 M in water), and 2 mL of DMF/H_2O (1:1) was sealed in a 20 mL vial with the pH of 5.0 and heated at 85 ^oC for 12 h and 105 ^oC for 24 h. Block crystals were collected (70 % and 75 % yield based on $Ln(NO_3)_3 \cdot 6H_2O$). The agreement between the experimental and simulated PXRD patterns indicated the phase-purity of the as-synthesized product (see Supporting Information Figure S3), and the as-synthesized compounds **9-10** were insoluble in water and common organic solvents. ICP and elemental analysis (wt %) for **9**: Calcd: C, 18.94; H, 0.99; N, 5.52; S, 6.32, La, 27.38, K, 7.70. Found: C, 18.85; H, 0.93; N, 5.49; S, 6.25, La, 27.28, K, 7.42. For **10**: Calcd: C, 18.89; H, 0.99; N, 5.51; S, 6.30, Ce, 27.55; K, 7.69. Found: C, 18.76; H, 0.93; N, 5.34; S, 6.16, Ce, 27.32; K, 7.51. IR (KBr, cm^{-1}) for two compounds (4000-400 cm^{-1}): 3537 (br), 1630 (vs), 1572 (vs), 1457 (s), 1392 (s), 1319 (m), 1211 (m), 1103 (w), 1009 (w), 809 (s), 699 (m), 554 (m) (Figure S4).

Synthesis of Compounds 11-12.

A mixture of $Ln(NO_3)_3 \cdot 6H_2O$ (Ln = La and Ce, 0.039 mmol), H_2tdc (0.100 mmol), KOH (0.05 mL, 0.56 M in water), and 2 mL of DMF/H_2O (3:1) was sealed in a 20 mL vial with the pH of 4.0 and heated at 85 ^oC for 12 h. Block crystals were collected (73 % and 69 % yield based on $Ln(NO_3)_3 \cdot 6H_2O$). The agreement between the experimental and simulated PXRD patterns indicated the phase-purity of the as-synthesized product (see Supporting Information Figure S5), and as-synthesized compounds **11-12** were insoluble in water and common organic solvents. ICP and elemental analysis (wt %) for **11**: Calcd: C, 17.36; H, 0.49; N, 10.12; S, 11.59, La, 33.46. Found: C, 17.24; H, 0.41; N, 9.91; S, 10.95, La, 32.95. For **12**: Calcd: C, 17.31; H, 0.48; N, 10.09; S, 11.55, Ce, 33.66. Found: C, 17.17; H, 0.36; N, 9.85; S, 10.93, Ce, 32.96. IR (KBr, cm^{-1}) for two compounds (4000-400 cm^{-1}): 3619 (w), 3486 (br), 2933 (w), 1613 (vs), 1442 (s), 1385 (m), 1103 (m), 850 (s), 660 (m), 532 (m), 482 (m) (Figure S6).

X-ray Structure Determination and Structure Refinement.

Crystallographic data for **4** were collected on a Rigaku RAXIS-RAPID IP diffractometer by using graphite-monochromated Mo-Kα radiation (λ = 0.71073 Å), while other compounds were collected on a Bruker SMART APEX-II CCD diffractometer by using graphite-monochromated Mo-Kα radiation (λ = 0.71073 Å). Absorption corrections are applied by using SADABS. The structures were solved with direct methods and refined with full-matrix least-squares techniques on F^2 using the SHELXTL program package.[9] Then Non-hydrogen atoms were refined with anisotropic temperature parameters. The hydrogen atoms of the partial coordinated water molecules and the guest water molecules could not be located but are included in the formula. The final formula was derived from crystallographic data combined with elemental and thermogravimetric analysis data. Crystal data and detailed data collection and refinement of compounds **1-12** are summarized in Table S1. Topology information for compounds **1-12** was obtained using TOPOS 4.0.[10]

Results and discussion

Crystal Structure of 1-8

Single-crystal X-ray diffraction analysis reveals that compounds **1-8** crystallize in the monoclinic space group $C2/c$. Because compounds **1-8** are isostructural (type I), only the structure of **1** is described in detail. The asymmetric unit contains one crystallographically independent La atom, one K atom, two tdc^{2-} ligands, two coordinated and a half guest water molecules. The bridging water oxygen O2W is on twofold axis. La(1) atom and K(1) atom are all 9-coordinated and both of them have distorted monocapped square antiprism coordination environments (Figure S7). La(1) atom is coordinated with eight oxygen atoms from the carboxylic group of five tdc^{2-} ligands, and one oxygen atom from terminal water molecule. K(1) atom is coordinated with two nitrogen atoms and five oxygen atoms from five tdc^{2-} ligands, as well as two oxygen atoms from two water molecules. The La-O bond lengths vary from 2.467 (2) to 3.0159 (19) Å, the K-O bond lengths vary from 2.7044 (19) to 3.362 (3) Å, and the K-N bond lengths are 2.956 (2) and 2.958 (2) Å, respectively. Owing to the effect of lanthanide contraction, the Ce-O bonds in **2**, the Pr-O bonds in **3**, Nd-O bonds in **4**, the Sm-O bonds in **5**, the Eu-O bonds in **6**, the Gd-O bonds in **7**, and the Tb-O bonds in **8** (see Supporting Information Table S2), are slightly shorter than the corresponding La-O bonds in **1**.

In the structure of **1**, tdc^{2-} ligand possesses two coordination modes and as the bridging linker with the oxygen atoms coordinates with two adjacent La atoms. As a result, four tdc^{2-} ligands and two La atoms can be regarded as a secondary building unit (SBU) (Figure 1a). The SBUs, in which two ligands point toward the outer surface and form screw propeller shaped, are connected alternately by tdc^{2-} ligand to generate 1D infinite zigzag chains with the La-La distances being 4.488 and 4.566 Å, respectively (Figure 1b). Then these zigzag chains with the ring of thiadiazole in parallel each other are linked via K atoms to form 2D layers along the *a* axis (Figure S8), and finally, water molecules pillar the structure to a 3D framework (Figure 1c). The total solvent-accessible volume is estimated, using *PLATON*,[11] to be only 6.8%, which indicate the structure is condensed (Figure 1d). A topological method is performed to further analyze the framework of compound **1**. La^{3+}, which link two K$^+$ and two La^{3+} by tdc^{2-} ligand, can be regarded as 4-connected nodes. K$^+$, which link one K$^+$ and two La^{3+} by tdc^{2-} ligand, can be viewed as 3-connected nodes. Therefore, the framework can be described as a bimodal (3, 4)-connected **moc** network with two different T sites and two distinct tiles: $[4^2.8^2]$ and $[8^6]$ (Figure 1e, f).

Crystal Structure of 9-10

As the compounds **9** and **10** are isostructural (type II), only the structure of **9** is described in detail. The asymmetric unit contains one crystallographically independent La^{3+}, one K$^+$, one tdc^{2-} ligand, one Fac ligand, four coordinated and one guest water molecules. The Fac ligands lie about inversion centre. La(1) atoms with distorted bicapped dodecahedral geometry coordinate to ten oxygen atoms from the carboxylic group of three tdc^{2-} ligands and two Fac ligands, as well as a terminal water molecule. K(1) atoms with distorted dodecahedral geometry coordinate to two nitrogen atoms and four oxygen atoms from four tdc^{2-} ligands, one oxygen atom from a Fac ligand and the remaining oxygen atom from terminal water molecule, respectively (Figure S9). The La-O bond lengths vary from 2.412 (3) to 2.889 (3) Å, the K-O bond lengths vary from

2.631 (5) to 3.127 (3) Å, and the K-N bond lengths are 2.950 (3) and 2.954 (3) Å, respectively. Owing to the effect of lanthanide contraction, the Ce-O bonds in **10**, are slightly shorter than the corresponding La-O bonds in **9** (Table S3).

In the structure of compound **9**, tdc^{2-} ligand as 7-connectors coordinates to three La atoms and four K atoms, and exhibits only one coordination modes, it leads to the SBU composed of two La atoms and two tdc^{2-} ligands and differs from those in compounds **1-8** structure (Figure 2a). Analog to them, the SBUs are linked together to generate 1D zigzag chains along *a* axis with the La-La distance being 4.555 and 4.644 Å, respectively (Figure 2b), and the chains are further connected via K atoms to form 2D layers (Figure S10). Expectably, Fac ligands replace the bridging water molecules and pillar the 2D layers to 3D framework (Figure 2c), and a 1D tube with the opening size of 5.2×5.9 Å along the *b* axis is exhibited (point-to-point and including van der Waals radii, as shown in Figure 2d). The total solvent-accessible volume for compound **9** is up to 15.1% by *PLATON* estimated. Topologically, La^{3+} as the metal center connects to other four La^{3+} by ligands can be considered as a 4-connected node, and the framework can be finally simplified as **dia** topology with one T site and one tile: $[6^4]$ (Figure 2e, f).
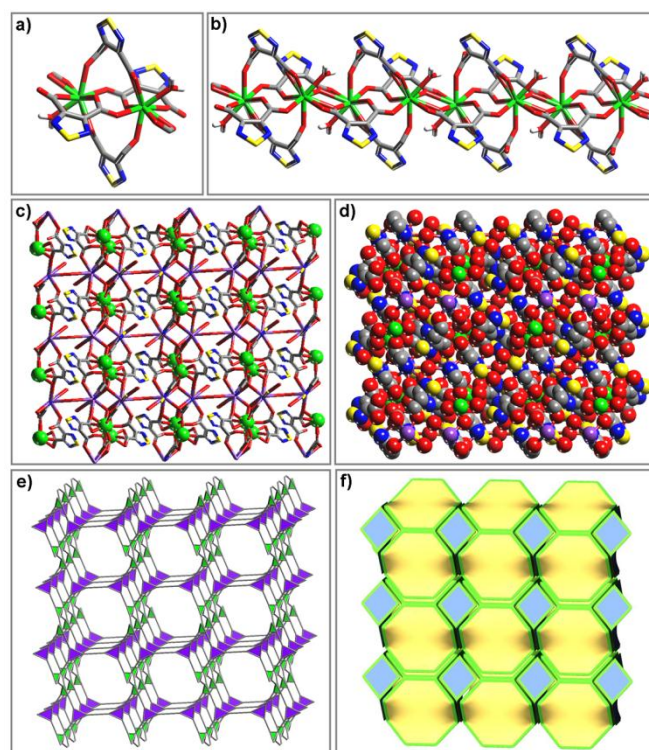
Figure 1. Description of the structures of **1-8**: a) the screw propeller shaped SBU; (b) presentation of the zigzag chain constructed by SBUs; c) stick model of the 3D framework along the [010] direction; d) space-filling representation of the 3D framework along the [010] direction; e) polyhedral view of the **moc** net; f) topological features displayed by tiling. Color scheme: carbon = gray, nitrogen = blue, oxygen = red, sulfur = yellow, lanthanide = green, potassium = purple.
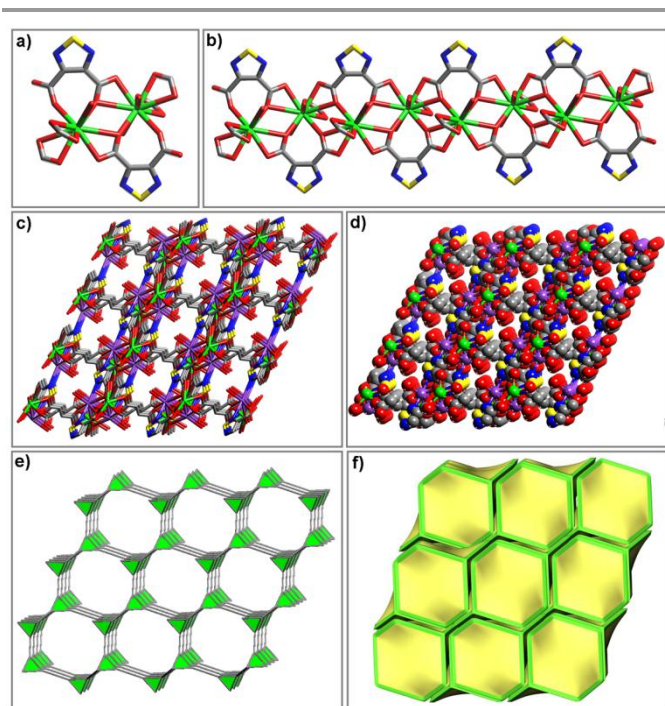
Figure 2. Description of the structures of **9** and **10**: a) SBU consisted of two ligand and two Ln atoms; (b) presentation of the zigzag chain constructed by SBUs; c) stick model of the 3D framework with a 1D channel along the [010] direction; d) space-filling representation of the 3D framework along the [010] direction; e) polyhedral view of the **dia** net; f) topological features displayed by tiling.

Crystal Structure of 11-12

Single-crystal X-ray diffraction analysis reveals that compounds **11** and **12** are isostructural (type III) and crystallize in the monoclinic $P2_1$ space group. Therefore, only the structure of **11** is described. Each asymmetric unit of **11** consists of two independent La^{3+} ions, three tdc^{2-} ligands, one coordinated and one guest water molecule. La(1) atoms, with $[LaN_4O_6]$ bicapped square antiprism geometry, coordinate with five tdc^{2-} ligands in a bidentate fashion through N, O-heterocoordination and O, O'- coordination mode, respectively. La(2) atoms, with $[LaN_2O_7]$ tricapped triprism geometry, are chelated by four tdc^{2-} ligand with the N, O - and O, O'-bidentate mode, as well as a terminal water molecule, respectively (Figure S11). The La-N bond lengths vary from 2.734 (6) to 2.847 (6) Å, the La-O bond lengths vary from 2.426 (5) to 2.585 (5) Å, respectively. Owing to the effect of lanthanide contraction, the Ce-N and Ce-O bonds in **12**, are slightly shorter than the corresponding La-N and La-O bonds in **11** (Table S4).

For compound **11**, tdc^{2-} ligand as a T-shaped linker coordinates with three La atoms. La centers are interconnected by bridging ligand to form 1D infinite left/right helical chains of $[La-tdc]_n$ running along the *b* axis with the same pitch of 12.9 Å (Figure 3), then the adjacent right/left chains are alternately linked to generate a 3D framework (Figure 4a). The resultant framework exhibits two types of channels along the *a* axis in which guests water reside (Figure 4b). Interestingly, five La atoms are interconnected by four tdc^{2-} ligands to produce a tetragonal pyramidal cage, and the cage links each other to compose a

triangle shaped channel with the opening size of 7.1×5.8 Å (Figure 4c), the other type of channel with a quadrangle shape has the openings with an approximate diameter of 7.6×5.3 Å in which the terminal water molecules protrude (point-to-point and including van der Waals radii). The total solvent-accessible volume for the compound **11** is estimated, using *PLATON*, to be 26.3%. From the viewpoint of the topology, the ligand, as a T-shaped linker, can be represented by a 3-connected triangle node, and the La(1) atom, which coordinates with five tdc^{2-} ligands, can be viewed as a trigonal bipyramidal node, La(2) atom, which coordinates with four tdc^{2-} ligands, can be regarded as a tetrahedron node (Figure 4d). Finally, the 3D structure of the compound **11** can be specified as a (3,4,5)-connected framework with a novel topology, and possesses three T sites and four tiles: $[6.8^2]$, $[6^4]$, $[6^2.8^2]$ and $[6.8^4]$ as shown in Figure 4e.
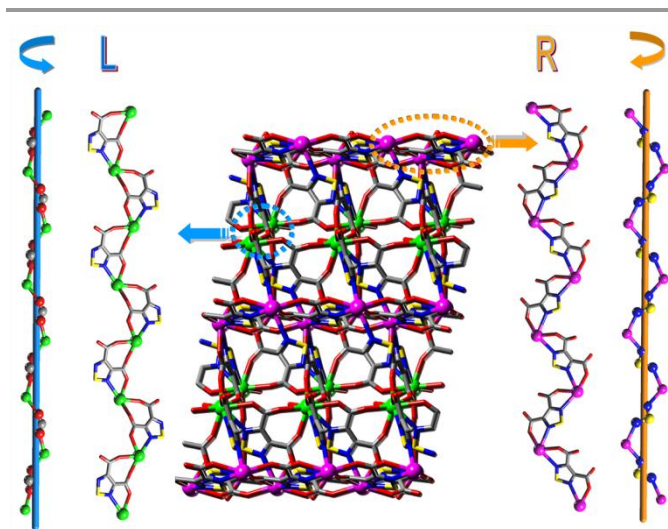
Figure 3. Stick model of the 3D framework with left/right helical chains in **11** and **12**.
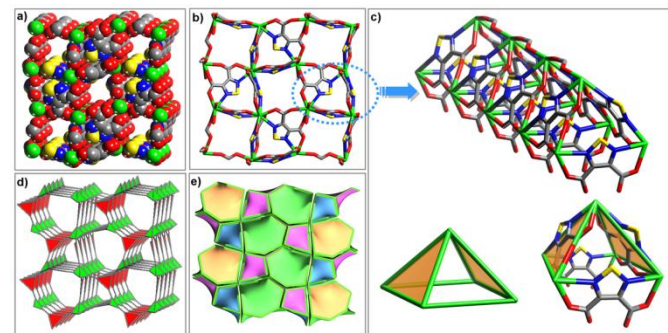
Figure 4. Description of the structures of **11** and **12**: a) space-filling representation of the 3D framework along the [100] direction; b) stick model of the 3D framework with two types of channels along the [100] direction; c) triangle shaped channels consisted of tetragonal pyramidal cage. d) polyhedral view of the net; e) topological features displayed by tiling.

Structural Diversity

As compounds **1-12** are synthesized in the similar reaction conditions, three types of structures from nonporous to open frameworks are exhibited. It provides a fair assessment of the critical influence of starting materials and solvent polarity. Compared with the reported MOFs based on the H_2tdc ligand (Figure 5a),[12] H_2tdc ligand has displayed four novel coordination modes in compounds **1-12**. For compounds **1-8**, the tdc^{2-} ligand adopts Figure 5b coordination mode and connects six metal atoms to form a 2D layer in *ab* plane, then the water molecules pillar the layers to 3D framework. The second coordination mode is exhibited by the tdc^{2-} ligand connecting four metal atoms to fill in the pores along *b* axis (Figure 5c). Because of the small molecule as the bridge linker and the tdc^{2-} ligand adopting the Figure 5c coordination mode, the structures of compounds **1-8** are condensed. Therefore, design to construct open-framework by introducing the second ligand as the bridging linker to replace pillared water molecule is performed. Fac, a linear shaped ligand as well as offering the hard donor atoms, is a good candidate for pillar. Simultaneously, the original reaction conditions are subtle changed which the relative molar ratio of $Ln(NO_3)_3·6H_2O$ and tdc^{2-} ligand from 1:2 to 1:1 to prevent the tdc^{2-} ligand from adopting the coordination mode as shown in Figure 5c. Because of the appreciably different radii of the Ln^{3+} ions, it causes only compound **9** for La^{3+} ions and compound **10** for Ce^{3+} ions to be obtained. Compared with the type I structure in compounds **1-8**, type II structure has the similar SBUs, and as expected, the tdc^{2-} ligand only adopts the Figure 5d coordination mode to form 2D layers, then the Fac ligands pillar the layers to form 3D open-framework. The total solvent-accessible volume of type II structure is estimated to be 15.1% which is higher than type I structure of 6.8%. As compounds **9** and **10** are successfully synthesized, a strategy to obtain diverse structure by modulating solvent polarity and the value of pH is carried out. Compared with the original reaction conditions, the volume ratio of DMF and H_2O is changed from 1:1 to 1:3 and the value of pH is modulated to be 4.0, then compounds **11** and **12** are synthesized with novel type III structure. Differ from the former, the tdc^{2-} ligand adopts only a single μ_3 in N, O- and O, O'-bidentate coordination mode to connect three Ln^{3+} ions as a T-shaped linker (Figure 5e). It leads to the structure distinctly differ from type I and II structures, and the total solvent-accessible volume is up to 26.3%. The structures of compounds **1-12** transforming from type I to type II and finally to type III indicate the important effect of starting materials, the solvent polarity and the value of pH during MOFs formation.
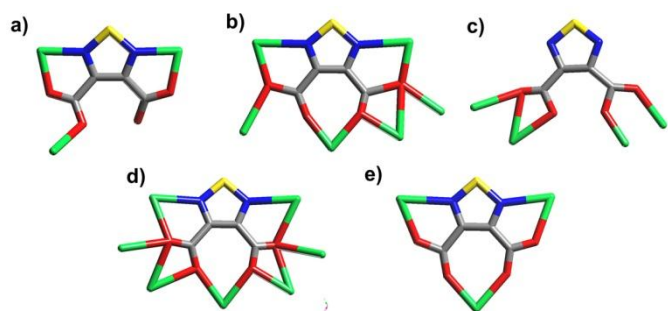
Figure 5. Five different coordination modes for tdc^{2-} ligand.

Thermogravimetric Analysis

Thermogravimetric analysis (TGA) measurements for compounds **1-12** indicate that compounds **1-8**, **9-10** and **11-12** display similar thermal performance due to their isomorphous structures, and they all exhibit high thermal stability as shown in Figure S12-S14. Thus, only the thermal stability of compound **1**, compound **9** and compound **11** are discussed in detail. TGA shows the framework of compound **1** is maintained till 300 °C. One-step weight loss of 7.1% is found before 200 °C, corresponding to the loss of guest and coordinated H_2O molecules (calcd: 7.9 %). On further heating, the H_2tdc ligand is decomposed accompanied by the collapse of the lattice structure in two process and loss weight of 51.8% between 300-800 °C. TGA for compound **9** shows that the framework is maintained till 300 °C. A two-step weight loss of 8.0 % is observed before 200 °C, corresponding to the loss of guest and coordinated H_2O molecules (calcd: 8.8 %). On further heating, a loss of 21.81 % between 300 and 360 °C should be corresponded to the release of part of the organic tdc^{2-} ligand. The further weight loss occurs from 360 to 800 °C (17.46%), and is assigned to the decomposition of the remaining tdc^{2-} ligand and the Fac ligand, according to the decomposition temperature of 400 °C for Fac ligand in the reported MOFs.[13] TGA indicates the structure of compound **11** is maintained till 320 °C, it shows one-step weight loss of 4.34 % between 170 and 320 °C, corresponding to the loss of guest and coordinated H_2O molecular (calcd: 4.33 %), between 320-730 °C, the H_2tdc ligand is decomposed accompanied by the collapse of the lattice structure in two process and loss weight of 49.19%.

Luminescent Properties

Taking into account the excellent luminescence property of Ln^{3+} and H_2tdc ligand in the visible region, compounds **1**, **5**, **6**, **7**, **8**, **9** and **11** are investigated in the solid state at room temperature. Two types of luminescence caused by different Ln^{3+} center and tdc^{2-} ligand are displayed, and some of them exhibit excellent luminescent properties with intense and narrow emission bands. As shown in Figure S15, the luminescence of ligand at room temperature exhibits a broad emission band between 450 and 550 nm with the emission maximum at 483 nm (excited at 397 nm, the excitation maximum).

The emission spectrum of compound **5** at λ_{ex} = 292 nm is shown in Figure 6a, in which four peaks at 560, 596, 642, and 704 nm are assigned to the $^4G_{5/2}{\rightarrow}^6H_{5/2}$, $^4G_{5/2}{\rightarrow}^6H_{7/2}$, $^4G_{5/2}{\rightarrow}^6H_{9/2}$, and $^4G_{5/2}{\rightarrow}^6H_{11/2}$ transitions of the Sm(III) ion. The $^4G_{5/2}{\rightarrow}^6H_{7/2}$ transition, as the strongest among the four bands, results in a strong orange luminescence, which is consistent with those found in previously reported Ln-MOFs.[4b, c, 14]

The emission spectrum of **6** (Figure 6b) at room temperature upon excitation at 260 nm exhibits the characteristic transition of Eu(III) ions, which can be attributed to $^5D_0{\rightarrow}^7F_J$ (J = 1, 2, 3, 4) transitions, *i.e.*, 592 nm ($^5D_0{\rightarrow}^7F_1$), 616 nm ($^5D_0{\rightarrow}^7F_2$), 654 nm ($^5D_0{\rightarrow}^7F_3$), and 700 nm ($^5D_0{\rightarrow}^7F_4$). Among these transitions, the $^5D_0{\rightarrow}^7F_2$ transition, which is hypersensitive to the coordination environment due to their strong electric dipole character, is the strongest one, leading to bright red luminescence. The $^5D_0{\rightarrow}^7F_1$ transition is a magnetic dipole transition; its intensity varies with the crystal field strength around the Eu(III) ions, the intensity ratio $I(^5D_0{\rightarrow}^7F_2)/I(^5D_0{\rightarrow}^7F_1)$ is about 4.5, which indicates that Eu(III) ions occupy sites with low symmetry and without an inversion center. This is in agreement with the result of the single-crystal X-ray analysis.

For **8**, the emission spectrum upon excitation at 368 nm shows the characteristic emission bands of Tb(III) at 490, 544, 584, 622, and 650 nm attributed to $^5D_4 \rightarrow {}^7F_J$ (J = 6, 5, 4, 3 and 2) transitions, *i.e.*, 490 nm ($^5D_4 \rightarrow {}^7F_6$), 544 nm ($^5D_4 \rightarrow {}^7F_5$), 584 nm ($^5D_4 \rightarrow {}^7F_4$), 622 nm ($^5D_4 \rightarrow {}^7F_3$), and 650 nm ($^5D_4 \rightarrow {}^7F_2$). The $^5D_4 \rightarrow {}^7F_6$ and $^5D_4 \rightarrow {}^7F_5$ emissions result from an electric dipole transition and a magnetic dipole transition, respectively. The $^5D_4 \rightarrow {}^7F_5$ transition, as the strongest among the four bands, results in a strong green luminescence output for the solid sample. The splitting for the peak at 584 nm is due to the crystal-field splitting (Figure 6c).

The luminescent properties of compounds **1**, **9** and **11** are shown in the Figure 6d, upon excitation at 356, 412 and 388 nm, respectively, compounds **1**, **9** and **11** are found to be luminescent with blue, green and blue emission maxima at 530, 478 and 548 nm. Because of the 4*f* orbit for La^{3+} is empty which leads to no *f-f* transition, the luminescence for **1**, **9** and **11** are assigned to an intraligand $\pi^* \rightarrow \pi$ transition since a similar emission at 483 nm is observed for the ligand. Analog to **1**, **9** and **11**, upon excitation at 338 nm, compound **7** is found to be luminescent with green emission maxima at 524 nm. Because of the 4*f* ^{7} configuration of Gd^{3+}, which has the extra stability of a half-filled shell, leading to the higher excitation level for *f-f* transition, therefore, the luminescence for compound **7** can be assigned to an intraligand fluorescent emission. The intensity increase of the luminescence for compounds **1**, **7**, **9** and **11** may be attributed to the chelation of the ligand to the metal center, which reduces the nonradiative relaxation process.[3a, 15]

From the luminescent spectra, these compounds exhibited two types of luminescence. As shown in Figure 6a-c, the ligands-based emission is not observed and Sm-, Eu- and Tb-compounds generate typical luminescent *f-f* emissions at visible region, it indicates that the ligand fully transforms the excitation energy to the 4*f* levels of the Ln^{3+}. It provides that the H$_2$tdc ligand could be as an excellent antenna organic linker to sensitize the Ln^{3+}. In addition, because of the exceptive configuration of La and Gd atoms, compounds **1**, **7**, **9**, and **11** exhibit luminescence with intense and broad emission bands which arising from intraligand $\pi^* \rightarrow \pi$ transition (Figure 6d).
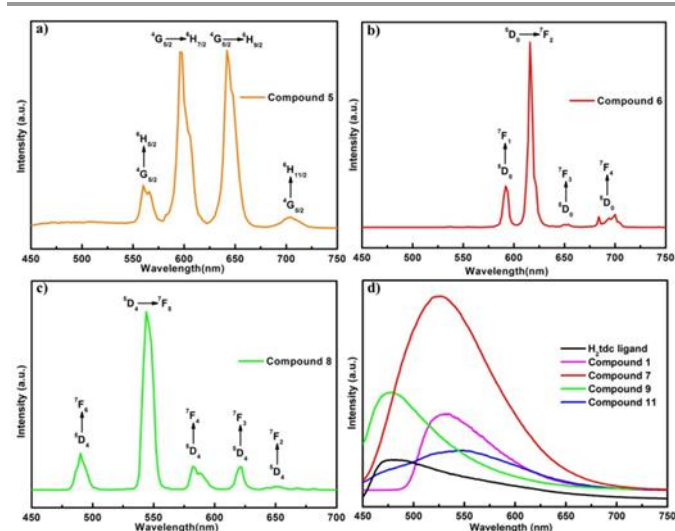
Figure 6. Solid state emission spectra of (a) 5, (b) 6, (c) 8 and (d) H2tdc ligand and 1, 7, 9, 11 collected at room temperature.

Conclusions

In conclusion, we have successfully assemble twelve novel Ln-MOFs possessing three types of structures with the **moc**, **dia** and a new (3,4,5)-connected topology based on the H$_2$tdc ligand. The H$_2$tdc ligand, as firstly reported with Ln-MOFs, exhibits four novel kinds of coordination modes, and it coordinates with lanthanide metal atoms to construct three unique types of structures by introducing the second ligand and modulating the polarity of the organic solvent. The total solvent-accessible volume of them is from 6.8% to 15.1% and finally to 26.3% indicating that the corresponding structures transferred from nonporous to more open framework. Luminescent property study shows that compounds **5**, **6**, and **8**, owing to the antenna effect of H$_2$tdc ligand, display intense orange, red and green luminescence and exhibits the typical Sm^{3+}, Eu^{3+} and Tb^{3+} ion emission. Meanwhile, compounds **1**, **7**, **9**, and **11** show intense green and blue luminescence due to the intraligand $\pi^* \rightarrow \pi$ transition. Obviously, the novel ligand H$_2$tdc will provide more diversity of coordination mode to construct new functional materials with various structures by selecting appropriate metal ions, and corresponding work is currently underway in our laboratory.

Acknowledgements

Notes and references

State key Laboratory of Inorganic Synthesis and Preparative Chemistry, Jilin University, Changchun, 130012, China. E-mail: zlr@jlu.edu.cn, yunling@jlu.edu.cn; Fax: +86-431-85168624; Tel: +86-431-85168614

† Electronic Supplementary Information (ESI) available: Powder XRD patterns, IR spectra, TGA curves, and PL spectrum, as well as some structure views of the twelve compounds. CCDC reference numbers 957579-957590. For ESI and crystallographic data in CIF or other electronic format See DOI: 10.1039/b000000x/

1 (a) M. Eddaoudi, J. Kim, N. Rosi, D. Vodak, J. Wachter, M. O'Keeffe and O. M. Yaghi, *Science*. 2002, **295**, 469-472; (b) H. Furukawa, N. Ko, Y. B. Go, N. Aratani, S. B. Choi, E. Choi, A. Ö. Yazaydin, R. Q. Snurr, M. O'Keeffe, J. Kim and O. M. Yaghi, *Science*. 2010, **329**, 424-428; (c) Z. Wang and S. M. Cohen, *Chem. Soc. Rev*. 2009, **38**, 1315-1329; (d) J. Lee, O. K. Farha, J. Roberts, K. A. Scheidt, S. T. Nguyen and J. T. Hupp, *Chem. Soc. Rev*. 2009, **38**, 1450-1459; (e) M. Kurmoo, *Chem. Soc. Rev*. 2009, **38**, 1353-1379.

2. (a) K. Sumida, D. L. Rogow, J. A. Mason, T. M. McDonald, E. D. Bloch, Z. R. Herm, T.-H. Bae and J. R. Long, *Chem. Rev*. 2011, **112**, 724-781; (b) R. B. Getman, Y.-S. Bae, C. E. Wilmer and R. Q. Snurr, *Chem. Rev*. 2011, **112**, 703-723; (c) J. S. Seo, D. Whang, H. Lee, S. I. Jun, J. Oh, Y. J. Jeon and K. Kim, *Nature*. 2000, **404**, 982-986; (d) Y. Liu, V. C. Kravtsov, R. Larsen and M. Eddaoudi, *Chem. Commun*. 2006, 1488-1490; (e) J.-R. Li, R. J. Kuppler, H.-C. Zhou, *Chem. Soc. Rev*. 2009, **38**, 1477-1504; (f) M. Kurmoo, *Chem. Soc. Rev*. 2009, **38**, 1353-1379; (g) W.-X. Zhang, W. Xue and X.-M. Chen, *Inorg. Chem*. 2010, **50**, 309-316; (h) F. Salles, G. Maurin, C. Serre, P. L. Llewellyn, C. Knöfel, H. J. Choi, Y. Filinchuk, L. Oliviero, A. Vimont, J. R. Long and G. Férey, *J. Am. Chem. Soc*. 2010, **132**, 13782-13788; (i) M. D. Allendorf, C. A. Bauer, R. K. Bhakta and R.

J. T. Houk, *Chem. Soc. Rev*. 2009, **38**, 1330-1352; (j) P. Horcajada, C. Serre, M. Vallet-Regí, M. Sebban, F. Taulelle and G. Férey, *Angew. Chem., Int. Ed*. 2006, **45**, 5974-5978; (k) Q. Chen, Z. Chang, W.-C. Song, H. Song, H.-B. Song, T.-L. Hu and X.-H. Bu, *Angew. Chem., Int. Ed*. 2013, **52**, 11550-11553.

3.　(a) X. Li, B.-L. Wu, C.-Y. Niu, Y.-Y. Niu and H.-Y. Zhang, *Cryst. Growth Des*. 2009, **9**, 3423-3431; (b) Y.-Q. Sun, J. Zhang, Y.-M. Chen and G.-Y. Yang, *Angew. Chem., Int. Ed*. 2005, **44**, 5814-5817; (c) C. Serre, F. Millange, C. Thouvenot, N. Gardant, F. Pelle and G. Ferey, *J. Mater. Chem*. 2004, **14**, 1540-1543; (d) J.-M. Jia, S.-J. Liu, Y. Cui, S.-D. Han, T.-L. Hu and X.-H. Bu, *Cryst. Growth Des*. 2013, **13**, 4631-4634; (e) X.-H. Bu, W. Weng, M. Du, W. Chen, J.-R. Li, R.-H. Zhang and L.-J. Zhao, *Inorg. Chem*. 2002, **41**, 1007-1010; (f) R. Yu, D. Wang, S. Ishiwata, T. Saito, M. Azuma, M. Takano, Y. Chen and J. Li, *Chem. Lett*. 2004, **33**, 458-459; (g) R. Yu, D. Wang, Y. Chen, X. Xing, S. Ishiwata, T. Saito and M. Takano, *Chem. Lett*. 2004, **33**, 1186-1187; (h) L. Li, R. Yu, D. Wang, X. Lai, D. Mao and M. Yang, *Inorg. Chem. Commun*. 2010, **13**, 831-833.

4.　(a) J. Xu, J. Cheng, W. Su and M. Hong, *Cryst. Growth Des*. 2011, **11**, 2294-2301; (b) W.-G. Lu, D.-C. Zhong, L. Jiang and T.-B. Lu, *Cryst. Growth Des*. 2012, **12**, 3675-3683; (c) Z.-G. Gu, H.-C. Fang, P.-Y. Yin, L. Tong, Y. Ying, S.-J. Hu, W.-S. Li and Y.-P. Cai, *Cryst. Growth Des*. 2011, **11**, 2220-2227.

5.　(a) T. Panda, P. Pachfule and R. Banerjee, *Chem. Commun*. 2011, **47**, 7674-7676; (b) M. Chen, M.-S. Chen, T.-A. Okamura, M.-F. Lv, W.-Y. Sun and N. Ueyama, *CrystEngComm*. 2011, **13**, 3801-3810.

6.　(a) T. K. Maji, G. Mostafa, H.-C. Chang and S. Kitagawa, *Chem. Commun*. 2005, 2436-2438; (b) Y.-Q. Sun, J. Zhang and G.-Y. Yang, *Chem. Commun*. 2006, 4700-4702.

7.　B. D. Chandler, D. T. Cramb and G. K. H. Shimizu, *J. Am. Chem. Soc*. 2006, **128**, 10403-10412.

8.　G. G., R. Ribaldone, *German Pat*. 1977, 2651604.

9.　G. M. Sheldrick, *SHELXTL-NT, version 5.1*. Bruker AXS Inc: Madison, WI, 1997.

10.　V. S. A. Blatov, V. Serezhkin and D. Korchagin, http://www.topos.ssu.samara.ru.

11.　A. L. J. Spec, *Appl. Crystallogr*. 2003, **36**, 7-13.

12.　J.-R. Li, Q. Yu, Y. Tao, X.-H. Bu, J. Ribas and S. R. Batten, *Chem. Commun*. 2007, 2290-2292.

13.　Z. Amghouz, L. Roces, S. García-Granda, J. R. García, B. Souhail, L. Mafra, F.-n. Shi and J. Rocha, *J. Solid State Chem*. 2009, **182**, 3365-3373.

14.　(a) Q.-B. Bo, H.-Y. Wang, D.-Q. Wang, Z.-W. Zhang, J.-L. Miao and G.-X. Sun, *Inorg. Chem*. 2011, **50**, 10163-10177; (b) Z.-J. Lin, Z. Yang, T.-F. Liu, Y.-B. Huang and R. Cao, *Inorg. Chem*. 2012, **51**, 1813-1820.

15.　(a) T.-T. Zhao, X.-M. Jing, J. Wang, D.-M. Wang, G.-H. Li, Q.-S. Huo and Y.-L. Liu, *Cryst. Growth Des*. 2012, **12**, 5456-5461; (b) Y. Cui, Y. Yue, G.-D. Qian and B.-L. Chen, *Chem. Rev*. 2011, **112**, 1126-1162.

Rational Design and Synthesis of a Series of 3D Lanthanide Metal-Organic Frameworks with Different Structures Driven by Reaction Conditions

Tingting Zhao, Lirong Zhang*, Dongmei Wang, Guanghua Li, Qisheng Huo, and Yunling Liu*

A series of novel lanthanide metal-organic frameworks with three types of structures, **moc**, **dia** and a new topology, have been constructed and their luminescent properties are investigated.